

ChmlsQ2b-04/27
BAD 2044, version 7

Collaboration-Wide Review
13 July 2008 to 24 July 2008

Primary BAD	2044, version 7 Search for B^+ meson decay to $a_1^+ K^0$
Author list	Merkel, Jesko
Review Committee	comm401, members: Gaz, Alessandro; Liu, Feng; Lombardo, Vincenzo (chair)
Target	2008 - 34th International Conference on High Energy Physics
Result type	
Supporting BAD(s)	BAD #1916 Search for the decay $B^+ \rightarrow a_1^+ K^0$
Changes since preliminary result	
BAIS/CWR Comments	
Institutional Reading Groups	2b. Budker, UCLA, Colorado, Royal Holloway, McGill, MIT, Trieste

Search for B^+ -meson decay to $a_1^+ K^{*0}$

6

The *BABAR* Collaboration

7

July 12, 2008

8

9

Abstract

10

We present the result of the search for the decay $B^\pm \rightarrow a_1^\pm K^{*0}$. The data, collected with the *BABAR* detector at the Stanford Linear Accelerator Center, represent 465 million $B\bar{B}$ pairs produced in e^+e^- annihilation at the $\Upsilon(4S)$ energy. The result for the branching fraction is, in units of 10^{-6} ,

11

12

13

$$\mathcal{B}(B^+ \rightarrow a_1^+ K^{*0}) \times \mathcal{B}(a_1^+ \rightarrow \pi^+ \pi^- \pi^+) = 0.7_{-0.5}^{+0.4+0.7} (< 1.6).$$

The first error quoted is statistical, the second systematic, and the upper limit in parentheses indicates the 90% confidence level.

14

15

Submitted to the 33rd International Conference on High-Energy Physics, ICHEP 08,
30 July—5 August 2008, Philadelphia, Pennsylvania.

16

17

Stanford Linear Accelerator Center, Stanford University, Stanford, CA 94309

18

Work supported in part by Department of Energy contract DE-AC02-76SF00515.

19

1 INTRODUCTION

Recent searches for decays of B mesons to final states with an axial-vector meson a_1 or b_1 and a pion or kaon have revealed modes with branching fractions that are rather large among charmless decays: $(15 - 35) \times 10^{-6}$ for $B \rightarrow a_1(\pi, K)$ [1, 2], and $(7 - 11) \times 10^{-6}$ for charged pion and kaon in combination with a b_1^0 or a b_1^+ meson [3, 4]. On the other hand the experimental search for $B^0 \rightarrow b_1^- \rho^+$ set an upper limit of 1.7×10^{-6} at 90% confidence level for the branching fraction [5], while a branching fraction of 25×10^{-6} was expected [6]. In this paper we present the first search at the *BABAR* experiment for the decay $B^+ \rightarrow a_1^+ K^{*0}$.

The available theoretical estimates of the branching fractions of B^+ meson to $a_1^+ K^{*0}$ come from calculations based on naïve factorization [7], and on QCD factorization [6]. The latter incorporates light-cone distribution amplitudes evaluated from QCD sum rules, and predicts branching fractions in quite good agreement with the measurements for $B \rightarrow b_1 \pi^+$ and $B \rightarrow b_1 K^+$ [3]. The expected branching fractions for $B^+ \rightarrow a_1^+ K^{*0}$ from calculations based on naïve factorization is 0.51×10^{-6} and for the calculation based on QCD factorization $9.7_{-3.5}^{+4.9+32.9} \times 10^{-6}$ with a prediction for the longitudinal polarization fraction f_L of $0.38_{-0.40}^{+0.51}$. The first theoretical error correspond to the uncertainties due to variation of Gegenbauer moments, decay constants, quark masses, form factors and a B meson wave function parameter. The second theoretical error correspond to the uncertainties due to variation of penguin annihilation parameters. For the longitudinal polarization fraction all errors are added in quadrature as the theoretical uncertainty is dominated by latter error. This mode is expected to be substantially enhanced by penguin annihilation and thus it is important to study this mechanism.

2 THE *BABAR* DETECTOR AND DATASET

The data for this measurement were collected with the *BABAR* detector [8] at the PEP-II asymmetric e^+e^- collider located at the Stanford Linear Accelerator Center. An integrated luminosity of 424 fb^{-1} , corresponding to $(465 \pm 5) \times 10^6 B\bar{B}$ pairs, was produced by e^+e^- annihilation at the $\Upsilon(4S)$ resonance (center-of-mass energy $\sqrt{s} = 10.58 \text{ GeV}$). Charged particles from the e^+e^- interactions are detected, and their momenta measured, by a combination of five layers of double-sided silicon microstrip detectors and a 40-layer drift chamber, both operating in the 1.5 T magnetic field of a superconducting solenoid. Photons and electrons are identified with a CsI(Tl) electromagnetic calorimeter (EMC). Further charged particle identification (PID) is provided by the average energy loss (dE/dx) in the tracking devices and by an internally reflecting ring imaging Cherenkov detector (DIRC) covering the central region. A detailed Monte Carlo program (MC) is used to simulate the B production and decay sequences, and the detector response [9].

Exclusive signal MC events are simulated as $B^+ \rightarrow a_1^+ K^{*0}$ with $a_1^+ \rightarrow \rho^0 \pi^+$. For the $a_1(1260)$ meson parameters we take the mass of $1230 \text{ MeV}/c^2$ and the width of $400 \text{ MeV}/c^2$. We account for the uncertainties of these resonance parameters in the determination of systematic uncertainties. The $a_1^+ \rightarrow \pi^- \pi^+ \pi^+$ decay proceeds mainly through the intermediate states $(\pi\pi)_{\rho\pi}$ and $(\pi\pi)_{\sigma\pi}$ [10]. No attempt is made to separate contributions of the dominant P-wave $(\pi\pi)_{\rho}$ from the S-wave $(\pi\pi)_{\sigma}$ in the channel $\pi\pi$. A systematic uncertainty related to the difference in the selection efficiency is estimated.

3 ANALYSIS METHOD

60

a_1^+ candidates are reconstructed through the decay sequence $a_1^+ \rightarrow \rho^0 \pi^+$ and $\rho^0 \rightarrow \pi^+ \pi^-$. The other primary daughter of the B meson is reconstructed as $K^{*0} \rightarrow K^+ \pi^-$. For the ρ^0 , the invariant mass of the pion pair is required to lie between 0.55 and 1.0 GeV/ c^2 , removing the peaking background component in the lower region of the distribution. For the a_1 and K^* , whose masses are treated as observables in the maximum likelihood (ML) fit described below, we accept a range that includes sufficiently wide sidebands. The a_1 invariant mass of the $\rho^0 \pi^+$ combination is required to lie between 0.9 and 1.8 GeV/ c^2 , where the K^* invariant mass of the $K^- \pi^+$ combination is required to lie between 0.8 and 1.0 GeV/ c^2 . Secondary charged pions from a_1 and K^* decays are rejected if classified as protons, kaons, or electrons by their DIRC, dE/dx , and EMC PID signatures. We reconstruct the B -meson candidate by combining the four-momenta of a pair of primary daughter mesons, using a fit that constrains all particles to a common vertex. From the kinematics of $\Upsilon(4S)$ decay we determine the energy-substituted mass $m_{\text{ES}} = \sqrt{\frac{1}{4}s - \mathbf{p}_B^2}$ and energy difference $\Delta E = E_B - \frac{1}{2}\sqrt{s}$, where (E_B, \mathbf{p}_B) is the B -meson four-momentum vector, and all values are expressed in the $\Upsilon(4S)$ rest frame. We require $5.25 \text{ GeV} < m_{\text{ES}} < 5.29 \text{ GeV}$ and $|\Delta E| < 100 \text{ MeV}$.

We also impose restrictions on the helicity-frame decay angle θ_{K^*} of the K^* mesons. The helicity frame of a meson is defined as the rest frame of the meson with the z axis along the direction of boost to that frame from the parent rest frame. For the decay $K^* \rightarrow K\pi$, θ_{K^*} is the polar angle of the daughter kaon, and for $a_1 \rightarrow \rho\pi$, θ_{a_1} is the polar angle of the normal to the a_1 decay plane. We define $\mathcal{H}_i = \cos(\theta_i)$, where $i = (K^*, a_1)$. Since many background candidates accumulate near $|\mathcal{H}_{K^*}| = 1$, we require $-0.98 \leq \mathcal{H}_{K^*} \leq 0.8$. The distributions \mathcal{H}_i are treated as observables in the maximum likelihood fit described later on.

Backgrounds arise primarily from random combinations of particles in continuum $e^+e^- \rightarrow q\bar{q}$ events ($q = u, d, s, c$). We reduce these with a requirement on the angle θ_{T} between the thrust axis [11] of the B candidate in the $\Upsilon(4S)$ frame and that of the charged tracks and neutral calorimeter clusters in the rest of the event (ROE). The distribution is sharply peaked near $|\cos \theta_{\text{T}}| = 1$ for jet-like continuum events, and nearly uniform for B -meson decays. The requirement, which optimizes the expected signal yield relative to its background-dominated statistical uncertainty, is $|\cos \theta_{\text{T}}| < 0.8$. $B\bar{B}$ background arising from $b \rightarrow c$ transition is suppressed by applying an appropriate veto against D-mesons.

The average number of candidates found per event in the selected sample is 1.5 (2.0 to 2.4 in signal MC depending on the polarization). We choose the candidate which is most likely a signal decay, judged from the output of a Neural Network, where we use the ρ meson mass, the B -, the a_1 - and the K_0^* fit probabilities as input variables.

In the ML fit we discriminate further against $q\bar{q}$ background with a Fisher discriminant \mathcal{F} that combines four variables: the polar angle of the B candidate momentum and of the B thrust axis with respect to the beam axis in the $\Upsilon(4S)$ rest frame; and the zeroth and second angular moments $L_{0,2}$ of the energy flow, excluding the B candidate, about the B thrust axis. The moments are defined by $L_j = \sum_i p_i \times |\cos \theta_i|^j$, where θ_i is the angle with respect to the B thrust axis of a track or neutral cluster i , p_i is its momentum, and the sum excludes the B candidate daughters.

We obtain yields and longitudinal polarization f_L from an extended ML fit with the input observables ΔE , m_{ES} , \mathcal{F} , the resonance masses m_{a_1} and m_{K^*} and the helicity distributions \mathcal{H}_{K^*} and \mathcal{H}_{a_1} . The number of events which pass the selection is 15802. Besides the signal events these samples contain $q\bar{q}$ (dominant) and $B\bar{B}$ with $b \rightarrow c$ combinatorial background, and a fraction of

104 other charmless $B\bar{B}$ background modes. The likelihood function is

$$\mathcal{L} = \exp\left(-\sum_j Y_j\right) \prod_i \sum_j Y_j \times \mathcal{P}_j(m_{\text{ES}}^i) \mathcal{P}_j(\mathcal{F}^i) \mathcal{P}_j(\Delta E^i) \mathcal{P}_j(m_{a_1}^i) \mathcal{P}_j(m_{K^*}^i) \mathcal{P}_j(\mathcal{H}_{K^*}^i) \mathcal{P}_j(\mathcal{H}_{a_1}^i), \quad (1)$$

105 where N is the number of events in the sample, and for each component j (signal, $q\bar{q}$ background,
106 $b \rightarrow c B\bar{B}$ background, or charmless $B\bar{B}$ background), Y_j is the yield of component j and $\mathcal{P}_j(x^i)$
107 is the probability for variable x of event i to belong to component j .

108 Since the correlation between the observables in the selected data and in MC signal events is
109 small, we take the probability density function (PDF) for each event to be a product of the PDFs
110 for the individual observables. Corrections for the effects of possible correlations are made on the
111 basis of MC studies described later.

112 We determine the PDFs for the signal and $B\bar{B}$ background components from fits to MC samples.
113 We develop PDFs for the combinatorial background with fits to the data from which the signal
114 region ($5.26 \text{ GeV} < m_{\text{ES}} < 5.29 \text{ GeV}$ and $|\Delta E| < 60 \text{ MeV}$) has been excluded.

115 The helicity part of PDF for signal component is the appropriate joint ideal angular distribution
116 from [12], multiplied by an empirical acceptance function $\mathcal{G}(\mathcal{H}_{K^*}, \mathcal{H}_{a_1})$.

117 The functions \mathcal{P}_j are constructed as linear combinations of Gaussian and polynomial functions,
118 relativistic Breit Wigner in case of resonance masses or in the case of m_{ES} for $q\bar{q}$ background, the
119 threshold function $x\sqrt{1-x^2} \exp[-\xi(1-x^2)]$, with argument $x \equiv 2m_{\text{ES}}/\sqrt{s}$ and shape parameter
120 ξ . These functions are discussed in more detail in [13], and are illustrated in Figure 1.

121 We allow the most important parameters for the determination of the combinatorial background
PDFs to float in the fit, along with the yields for the signal and $q\bar{q}$ background. We validate the

Table 1: Summary of results for $B^+ \rightarrow a_1^+ K^{*0}$. Signal yield Y , fit bias Y_b , product branching fraction $\prod \mathcal{B}_i$, significance S , branching fraction \mathcal{B} and upper limit UL. The given uncertainties on fit yields are statistical only, the uncertainties on the fit bias include the corresponding systematic uncertainties.

Y	Y_b	$\prod \mathcal{B}_i$	S	$\mathcal{B}(10^{-6})$	UL (10^{-6})
55_{-17}^{+19}	27 ± 14	$\frac{2}{3}$	0.9	$0.7_{-0.5}^{+0.4+0.7}$	1.6

122 fitting procedure by applying it to ensembles of simulated experiments with the $q\bar{q}$ component drawn
123 from the PDF, into which we have embedded known numbers of signal and $B\bar{B}$ background events
124 randomly extracted from the fully simulated MC samples. By tuning the number of embedded
125 events until the fit reproduces the yields found in the data, we determine the bias that is reported,
126 along with the signal yield, in Table 1. We fixed $f_L = 1$ to extract the branching fraction to achieve
127 the most conservative upper limit. In the above procedure we allowed f_L to vary in the fit and
128 found the value $f_L = 1.1 \pm 0.2$, we quoted only the statistical error since, given that we do not
129 observe any significant signal, we do not report the measured value of f_L .

130 In Figure 1 we show the projections of data with the PDF overlaid. The data plotted are
131 subsamples enriched in signal with the requirement of a minimum value of the ratio of signal to
132 total likelihood (computed without the plotted variable).
133

We compute the branching fraction by subtracting the fit bias from the measured yield, and dividing the result by the number of produced $B\bar{B}$ pairs and by the efficiency times $\mathcal{B}(K^{*0} \rightarrow K^+\pi^-) = \frac{2}{3}$. The efficiency is obtained from the MC signal model. The efficiency for longitudinally and transversally polarized signal events is 12.9% and 18.6%, respectively. We assume that the branching fractions of the $\Upsilon(4S)$ to B^+B^- and $B^0\bar{B}^0$ are equal, consistent with measurements [10]. The results are given in Table 1, along with the significance, computed as the square root of the difference between the value of $-2\ln\mathcal{L}$ (with additive systematic uncertainties included) for zero signal and the value at its minimum.

4 SYSTEMATIC STUDIES

Systematic uncertainties on the branching fractions arise from the imperfect knowledge of the PDFs, $B\bar{B}$ backgrounds, fit bias, and efficiency. PDFs uncertainties not already accounted for by free parameters in the fit are estimated from varying the signal-PDF parameters within their uncertainties. For resonance mass parameters we use the uncertainties from [10]. The uncertainty from fit bias (Table 1) includes its statistical uncertainty from the simulated experiments, and half of the correction itself, added in quadrature. For the $B\bar{B}$ backgrounds we vary the fixed fit component by 100% for charmless background and by 20% for the charm background.

In the systematic uncertainty we account for a possible $B^+ \rightarrow a_2^+ K^{*0}$ contribution by parameterizing its PDFs on a dedicated sample of simulated events; for the helicity part of this component we use the corresponding joint ideal angular distribution from [12], as we do for our signal component. We vary the $B^+ \rightarrow a_2^+ K^{*0}$ yield from 0 to 19 events, based on a branching fraction of 0.7×10^{-6} . We are not aware of any theoretical prediction or assumption for this branching fraction, but the general belief obtained from other charmless B decays involving a_1 mesons is that a $B^+ \rightarrow a_2^+ K^{*0}$ decay is suppressed with respect to $B^+ \rightarrow a_1^+ K^{*0}$. We conservatively assume $B^+ \rightarrow a_2^+ K^{*0}$ branching ratio could be as large as the $B^+ \rightarrow a_1^+ K^{*0}$.

The uncertainty from the polarization is obtained by varying f_L within their error found in studies where f_L was allowed to vary in the fit. Uncertainties in our knowledge of the tracking efficiency include 0.3% per track in the B candidate. The uncertainties in the efficiency from the event selection are below 0.6%. We determine the systematic uncertainty on the determination of the integrated luminosity to be 1.1%. All Systematic uncertainties on the branching fraction are summarized in Table 2.

5 RESULTS

We obtain for the branching fraction (in units of 10^{-6}):

$$\mathcal{B}(B^+ \rightarrow a_1^+ K^{*0}) \times \mathcal{B}(a_1^+ \rightarrow \pi^+\pi^-\pi^+) = 0.7_{-0.5}^{+0.4+0.7}_{-0.7} (< 1.6).$$

The first error quoted is statistical and the second systematic. We find no evidence for $B^+ \rightarrow a_1^+ K^{*0}$ decay; we find a significance of 0.9 standard deviations, therefore we quote a 90% confidence level upper limit, given in parentheses.

The upper limit from this measurement is on the one hand in agreement with the prediction from naïve factorization [7] and on the other hand significantly lower than the QCD factorization estimation [6], but within the experimental and theoretical uncertainties not sufficiently to completely rule it out.

Table 2: Summary of systematic uncertainties of the determination of the $B^+ \rightarrow a_1^+ K^{*0}$ branching fraction.

Source of systematic uncertainty	
Additive errors (events)	
$b \rightarrow c B\bar{B}$ background	6
Charmless $B\bar{B}$ background	12
$B^+ \rightarrow a_2^+ K^{*0}$ background	14
Parametrization for a_1 meson	4
PDF parametrization	3
Variation on f_L	2
ML Fit Bias	14
Total additive (events)	26
Multiplicative errors (%)	
Tracking efficiency	1.2
Determination of the integrated luminosity	1.1
MC statistic (signal efficiency)	0.6
Differences in the selection efficiency for the a_1 decay	3.3
Particle identification (PID)	1.4
Event shape restriction ($\cos \theta_T$)	1.0
Total multiplicative (%)	4.1
Total systematic error [$\mathcal{B}(10^{-6})$]	± 0.7

6 ACKNOWLEDGMENTS

We are grateful for the extraordinary contributions of our PEP-II colleagues in achieving the excellent luminosity and machine conditions that have made this work possible. The success of this project also relies critically on the expertise and dedication of the computing organizations that support *BABAR*. The collaborating institutions wish to thank SLAC for its support and the kind hospitality extended to them. This work is supported by the US Department of Energy and National Science Foundation, the Natural Sciences and Engineering Research Council (Canada), the Commissariat à l’Energie Atomique and Institut National de Physique Nucléaire et de Physique des Particules (France), the Bundesministerium für Bildung und Forschung and Deutsche Forschungsgemeinschaft (Germany), the Istituto Nazionale di Fisica Nucleare (Italy), the Foundation for Fundamental Research on Matter (The Netherlands), the Research Council of Norway, the Ministry of Education and Science of the Russian Federation, Ministerio de Educación y Ciencia (Spain), and the Science and Technology Facilities Council (United Kingdom). Individuals have received support from the Marie-Curie IEF program (European Union) and the A. P. Sloan Foundation.

References

- [1] *BABAR* Collaboration: B. Aubert *et al.*, Phys. Rev. Lett. **97**, 051802 (2006); Phys. Rev. Lett. **99**, 261801 (2007).

- [2] *BABAR* Collaboration: B. Aubert *et al.*, Phys. Rev. Lett. **100**, 051803 (2008).
- [3] *BABAR* Collaboration: B. Aubert *et al.*, Phys. Rev. Lett. **99**, 241803 (2007).
- [4] Charge-conjugate reactions are implied unless noted.
- [5] W. T. Ford for the *BABAR* Collaboration, presented at FPCP, Taipei, Taiwan (2008).
- [6] H. Cheng and K. Yang, arXiv:0805.0329v1 (2008).
- [7] G. Calderón, J. H. Munõz, and C. E. Vera, Phys. Rev. D **76**, 094019 (2007).
- [8] *BABAR* Collaboration: B. Aubert *et al.*, Nucl. Instrum. Methods Phys. Res., Sect. A **479**, 1 (2002).
- [9] The *BABAR* detector Monte Carlo simulation is based on GEANT4 [S. Agostinelli *et al.*, Nucl. Instrum. Methods Phys. Res., Sect. A **506**, 250 (2003)] and EvtGen [D. J. Lange, Nucl. Instrum. Methods Phys. Res., Sect. A **462**, 152 (2001)].
- [10] Particle Data Group: Y.-M. Yao *et al.*, J. Phys. **G33**, 1 (2006) and 2007 partial update for the 2008 edition.
- [11] A. de Rújula, J. Ellis, E. G. Floratos and M. K. Gaillard, Nucl. Phys. B **138**, 387 (1978).
- [12] A. Datta Phys. Rev. D **77**, 114025 (2008).
- [13] *BABAR* Collaboration: B. Aubert *et al.*, Phys. Rev. D **70**, 032006 (2004).

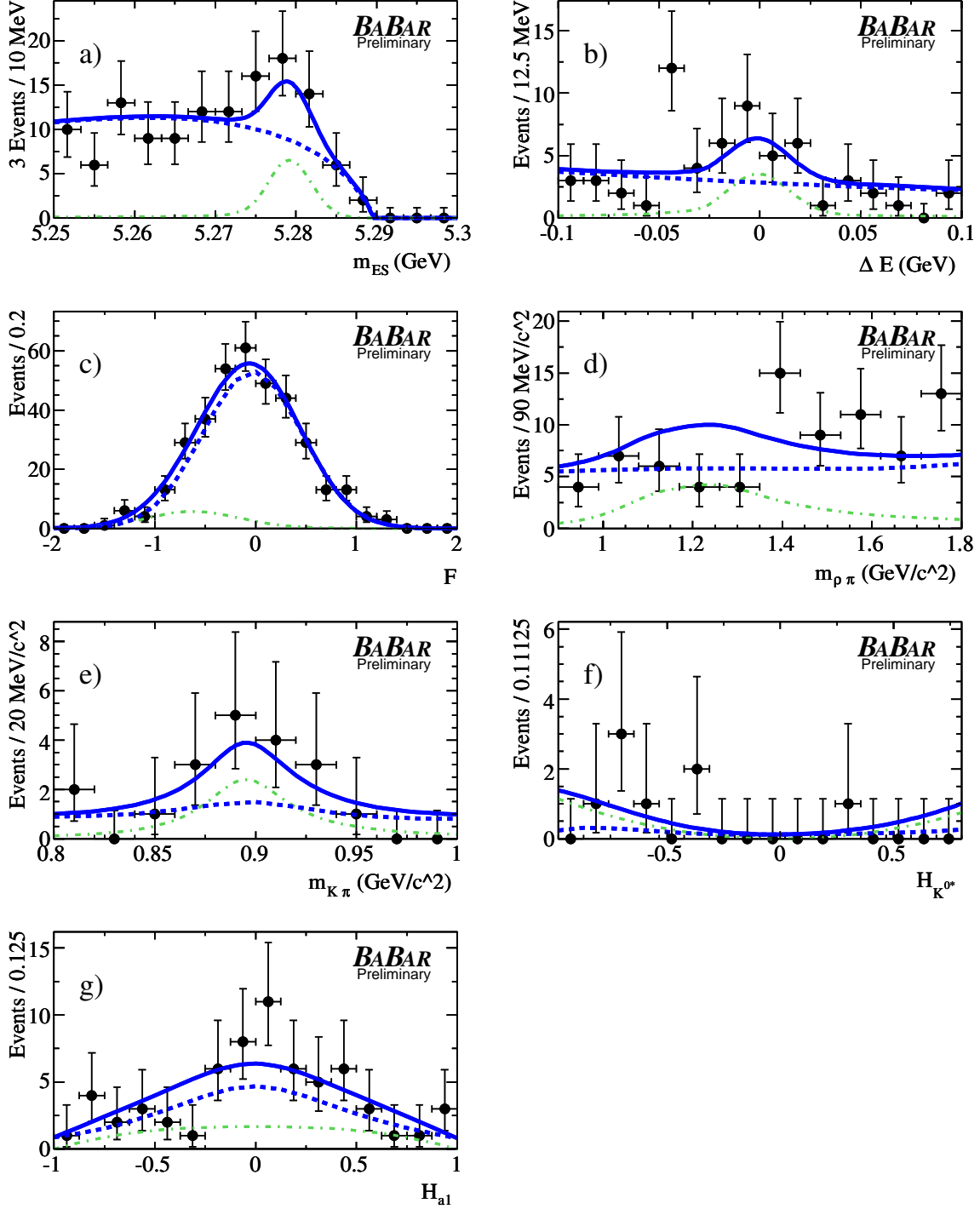


Figure 1: Distributions for signal-enhanced subsets (see text) of the data projected onto the fit observables for the decay $B^+ \rightarrow a_1^+ K^{*0}$; (a) m_{ES} , (b) ΔE , (c) \mathcal{F} , (d) $m(\rho\pi)$ for the a_1 candidate, (e) $m(K\pi)$ for the K^* candidate, (f) \mathcal{H}_{K^*} and (g) \mathcal{H}_{a_1} . The solid lines represent the results of the fit, and the dot-dashed and dashed lines the signal and background contributions respectively. These plots are made with cuts on the ratio of signal to total likelihood where 19% to 46% of signal events with respect to the nominal fit depending on the variable remain.